International Journal of Clinical and Experimental Medical Sciences
2016; 2(3): 40-51
http://www.sciencepublishinggroup.com/j/ijcems
doi: 10.11648/j.ijcems.20160203.12
ISSN: 2469-8024 (Print); ISSN: 2469-8032 (Online)

SciencePG
Science Publishing Group

Research Article

Assessment of Experimental Permanent Coronary Artery Ligation Using Echocardiography and Invasive Real-Time Pressure-Volume (PV): A Practical Tips to Evaluate Rat Hemodynamics

Filip Konecny

Department of Surgery, Division of Plastic Surgery, Microsurgery, McMaster University, Hamilton, Ontario, Canada

Email address:
fkonecny@uhnres.utoronto.ca
Corresponding author

To cite this article:
Filip Konecny. Assessment of Experimental Permanent Coronary Artery Ligation Using Echocardiography and Invasive Real-Time Pressure-Volume (PV): A Practical Tips to Evaluate Rat Hemodynamics. *International Journal of Clinical and Experimental Medical Sciences*. Vol. 2, No. 3, 2016, pp. 40-51. doi: 10.11648/j.ijcems.20160203.12

Received: April 26, 2016; **Accepted**: June 3, 2016; **Published**: June 20, 2016

Abstract: **Background:** Rat permanent coronary artery ligation is surgical model mimicking coronary artery ischemia and myocardial infarct (MI) injury, both sequels of coronary artery disease (CAD). The aim of this publication is to provide comprehensive, detailed description of rat load-dependent and independent hemodynamic assessment at baseline and at 28 days post-myocardial ischemia and remodeling. Materials and Methods: the detailed depiction of rat-MI model is followed by a thorough assessment of hemodynamics by two-dimensional (2D) echocardiography and invasive pressure-volume (PV) catheterization. Results: Quantification of post-MI using 2D M-mode showed a significant increase in end-systolic and end-diastolic dimensions with a decrease of fractional shortening. PV load-dependent hemodynamics at 28 days showed a rightward shift of PV loop on the volume axis, characterized by an increase of LVEDV; (319±73 vs. 215±79 µl; P<0.001) and the LVESV (157±39 vs. 57±28 µl; P<0.001). Both dpdtmax and ESP were significantly influenced by decreasing the number of myocytes, leading to a significant decrease of dpdtmax (5786±1443 vs. 9609±4126 mmHg; P<0.01) and ESP (91.5±12 vs. 108.2±13 mmHg; P<0.001). Loss of contractile myocytes had an effect on the cardiac output (CO) and ejection fraction (EF); (49±12 vs. 68±3.5 ml/min; P<0.05) and (50±8.5 vs. 76±4.9 % P<0.001). Diastolic dysfunction had a major influence on LV lusitropy at day 28 post-MI characterized by prolonged LV filling at higher LVEDP (9.1±2.9 vs. 5.18±2.5 % P<0.01), higher Tau values, time to peak filling and dpdt min (-4850±1062 vs. 5876±1443 mmHg; P<0.001). Using histopathology, calculated HW/BW ratio (g/mg) (3.1±0.22 vs. 3.82±0.39; P<0.001), reflected hypertrophy of post-remodeled myocardium. Conclusion: Heart failure (HF) post-permanent coronary artery ligation influences both systolic and diastolic hemodynamics. Comprehensive assessment of modeled HF using load-dependent and independent indices enables its clinical translation.

Keywords: Permanent Coronary Artery Ligation, Rat Model, Echocardiography, Invasive Pressure-Volume Hemodynamics

1. Coronary Artery Disease, Myocardial Infarction and Rat Model of Translation

The underlying cause of coronary artery ischemia and myocardial infarct (MI) is coronary artery disease (CAD). The hallmark of the disease is the presence of an acute thrombus overlying an atherosclerotic plaque within the coronary artery lumen. As plaque(s) grow they occlude blood flow or suddenly rupture initiating hemorrhage, coagulation and intraluminal thrombosis that is in most cases found post-mortem.[1] As delivery of nutrients and oxygen are acutely ceased myocardium endures irreversible damage that impairs overall energy metabolism in cardiac cells.

Historically, the rat model of MI dates back to 1946 when Heimburger described the coronary artery ligation to create

the MI.[2] The technique of MI induction changed throughout 70-ties[3,4] and became popular after Pfeffer et al described its current version.[5] This model enabled revolutionary observation that vasodilatation might relive the amount of LV load in post-infarcted heart and led to use and development of Ang II inhibitors[6]. Subsequent studies led to trials where Captopril or placebo was administered following MI in patients with reduced LV function.[7,8]

Clinical types of MI could be outlined as a) the non-reperfusion type, where the obstruction to blood flow is permanent, or b) the reperfusion-type if the obstruction is reversed. Furthermore, in the human scenario (either right or left coronary artery dominance) the anatomic variation plays a major role in the position and final size of ischemic necrosis. The left main coronary artery (LMCA) occlusion generally results in a large anterolateral infarct including the septum, whereas occlusion of the left anterior descending (LAD) coronary artery causes necrosis limited to the anterior wall. Rat MI modeling by the positioning of the occluding suture on the descending coronary artery can be correlated to the severity of the infarct seen in man. As reported by Chen et al[9] in the Sprague-Dawley (SD) rat, the infarct size mainly depends on the length and size of the injured branch, but not on the branch patterns.[9] The final infarct size might also be related to an ability to properly visualize the coronary artery, due to the variation of its position in rat and also because only about 24% is visible during the MI procedure.[9] In addition, observed by the same group, the severity of infarct has been related to suture occlusion-tightness. If the occlusion was not firm enough, a residual vessel tail was left in post-MI heart influencing the final infarct size.[9] Furthermore, outbred SD as compared to inbred Lewis rat shows a marked variability in infarct size with high post-MI mortality (36% vs. 16%).[10] Such limitation is in direct correlation with the occlusion of the coronary artery; hence differences captured by the infarct size measurement might just be an intrinsic variable of this model. The variability of ligature position, the length, tightness and the size of injured branch of the coronary artery are important factors to be considered while developing the rat MI model. Thus e.g. if the rat coronary artery is occluded too close to its origin, very close to the septal artery branch, it increases the infarct size leading to higher mortality.[11] For that reason, some authors instead of permanent coronary artery ligation decided to use cryoinjury model. Cryoinjury instigates MI by freezing the LV free wall for ~3 min with cryo-probe using temperatures of minus 160°C.[12,13] Cryoinjury technique has not replaced permanent coronary artery ligation, however, it is widely used to recapitulate and to study the engraftment of transplanted stem cells of e.g. mesenchymal origin post-MI alone[14] or incorporated into scaffolds.[15] Another limitation of the rat model of coronary artery ligation is that the procedure is frequently performed on males from following strains: SD, Wistar, Lewis, and Fisher. These young adults usually weighing between 250 to 300g at the study beginning and are healthy, well-adjusted to transport and other stressors while under the MI protocol.[9,10,16,17] Later, as they enter into the study, their health, age, and diet guarantee no-comorbidities while they are subjected to study as e.g. high blood pressure, atherosclerosis, smoking, diabetes mellitus, hypolipoproteinemia, abdominal obesity, which can be observed in the clinical setting. Moreover, there is not yet a genetic polymorphism study performed in a rat linking e.g. a common allele on chromosome 9 to be associated with coronary heart disease.[18,19] To recapitulate these pre-clinical conditions such as feeding cholesterol-rich diet to rodents has been proven to be challenging.[20] Currently, few training courses are available to develop necessary technical skills to perform an open chest cardiac surgeries in a rat, and few publications exist describing these rather complex catheterization procedures. To perform surgical procedures in a rat, investigators rely on brief methodical descriptions in articles and books. Later, they have to work out important details of the surgical model by trial and error. To gain these skills only through the experimental approach is frequently time-consuming, not always successful, and it repeatedly involves the loss of animals, resulting in the use of higher numbers to reach statistically significant results.

The aim of this publication is to provide a comprehensive description of the permanent coronary artery ligation, along with important pathophysiological measurements of heart function. Particularly, a detailed and expanded description of animal preparation for the surgery with steps leading to successful intubation along with three major procedures used in cardiovascular research have been provided: *1*) permanent coronary artery ligation leading to (LV myocardial infarct), *2*) echocardiography (non-terminal visualization technique), and *3*) heart hemodynamics (terminal pressure-volume measurement) with description provided for non- and post-injured LV. Additionally, researchers might find an interesting discussion about some of the load-independent parameters at the end of the publication and in Figure 6.

2. Material and Methods

2.1. Surgical Preparation and Anesthesia

All procedures described in this publication were performed in accordance with the National Institute of Health (NIH) standards and approved by the Institutional Animal Care and Use Committee of University Health Network (UHN). Before procedures, all animals were acclimatized for at least 3 days post-arrival. Animal weight, age, sex, and strain were marked into excel sheet before surgery. Triage of each animal was performed before an institution of general anesthesia and marked into excel sheet (respiratory rate 65-110 breaths/min), HR (305-500 beats/min) and temperature (38.1-38.5°C) taken using digital thermistor thermometer. Rats were pre-anaesthetized with 3-4% Isoflurane (Forane, Baxter, IL) mixed with fresh flowing Oxygen 0.5 l/min inhaled in the induction chamber with lid, undisturbed during induction. An ophthalmic ointment was applied to both eyes following induction of anesthesia to prevent corneal drying. Rats were shaved while on warming pad, using The Wahl® ChroMini Cordless Trimmer (Harvard

Apparatus, QC). The remaining fur was removed from the surgical area using depilatory cream Nair (Church & Dwight Co., Inc., Ewing, NJ). Surgical scrub used disinfectants i.e. iodophores, chlorhexidines, and alcohol. Rats were scrubbed in the pre-op room area separated from the surgery operation room. Later, animals were given 0.5 ml of pre-warmed 0.9% saline along with analgesics Buprenorphine (0.01-0.05 mg/kg) all i.p. Rats were transorally intubated using a 16-gauge polyethylene catheter (Insyte-W catheter, BD) with the help of fiberscope Fiber-lite (M-150) (Dolan-Jenner Industries, MA) by directly illuminating the ventral area of the neck. Volume ventilation was instituted via rodent ventilator Volume Controlled Ventilator 683 (Harvard Apparatus, QC) using tidal volumes and ventilation cycles per minute as per Table 1.

Table 1. *Calculated respiration rate and tidal volumes based on rat weight.*

Rat weight (g)	Respiration rate (breaths/min)	Tidal volume (ml)
250	77	1.53
265	76	1.62
285	74	1.74
300	73	1.84

When connected to low resistance non-rebreathing circuit, capillary refill time and breathing pattern was inspected. Post-induction anesthesia was adjusted to Isoflurane (2%) with animal placed on a water based circulating heating pad (Gaymar, Braintree, MA) set on "low heat" (38°C). Adequate anesthesia was accompanied by loss of muscle tone and by the loss of reflexes e.g. corneal, pinnae and pedal. Three leads skin surface ECG electrode configuration was selected to monitor heart rhythm.

2.2. Functional Two-Dimensional M-mode Echocardiography

Rats were pre-anaesthetized and kept on 1.5% of Isoflurane anesthesia. The left recumbent position was selected while on heating pad, with the temperature maintained at 38.0 ± 0.5 C°. Rat's left paw was stretched forward at about 60 ° angle and taped. Aquasonic 100 ultrasound transmission gel (Parker Inc., Fairfield, NJ) was warmed up. Vivid 7 system (GE Mississauga, ON) was used for the echocardiographic examinations equipped with 10 MHz linear transducer operated at a depth of 2 cm and a sectorial angle of 60° capable of producing images in the single dimensional or two-dimensional (2D) modes and of analyzing the intracardiac blood flow velocity with Doppler spectral analysis and color flow mapping techniques. American Society of Echocardiography guidelines[21] were followed to discriminate LV dimensions, wall thickness from a short-axis view at the level of the papillary muscles. At the beginning, longitudinal images of the heart including the LV and atrium, the mitral valve, and the aorta, followed by the cross-sectional images from the base plane from the aorta, the left atrium, the right ventricular outflow tract, to the left ventricular apical region were obtained. M-mode tracings of the aortic root, the mitral and pulmonary valves, and the LV cavity at the level of the papillary muscles were acquired. The following parameters were measured by M-mode tracings and averaged from 3 cardiac cycles: Left Ventricle End Diastolic Distance (LVEDD), Left Ventricle End Systolic Distance (LVESD), anterior and posterior wall thickness of systole and diastole. LVESD and LVEDD were used to derive end-diastolic volume as per Brown et al,[22] as follows (EDV)= 1.047 ×(LVEDD)^3 and the end-systolic volume (ESV)= 1.047 × (LVIDD)^3. Fractional Shortening (FS in %) was calculated according to the formula FS = [(LVEDD – LVEDS)/LVEDD] x 100. The imaging was performed by placing M-mode cursor at the level of the papillary muscles in a parasternal short axis view perpendicular to the septum and LV posterior wall. End-diastole was defined as frame after the mitral valve closure. The end systole was defined from the frame preceding the mitral valve opening. Furthermore due to post-MI LV cavity remodeling, adherence to as close as possible cursor placing to the papillary muscle area ensured proper acquisition. These sets of images were obtained with a depth setting of 2 cm and at a frame rate of ≥122 frames/s and a sweep speed of ~200 mm/s. After recording of M-mode tracings, pulsed Doppler was used at a velocity of 100mm/s simultaneously accompanied by the electrocardiogram. Digital images were stored for later review. The rat was allowed to recover at a low-traffic area away from the exam area, undisturbed warmed under a heating lamp.

2.3. Chamber Dimensions and Stroke Volume Determination

Pulsed wave (PW) Doppler was used to determine the velocity time integrals (VTI) at the LV outflow tract in the area of the aortic root in the parasternal long axis view. The aortic diameter was measured during systole and determined from the 2-D images. With the use of these measurements, stroke volume was calculated by using the formula: SV (ml) = D2*π/4*VTI $_{(LVOT)}$.[23, 24]

2.4. The Left Coronary Artery Permanent Suture Ligation

Animal's left paw was extended at about 90° angle and taped. The right paw was also moved forward and taped. The first scalpel incision was at an angle of 60° about 4-5 cm long, from the top of the axillar (armpit) area towards the left sternal border. Local anesthesia was applied subcutaneously to limit pain in the area. Muscles of the thoracic wall (external and internal intercostal mm. and transverse thoracic m.), were cut and separated. Attention was given to not to cut the internal mammary artery or vein running in the area, as it usually leads to profuse bleeding. The left thoracotomy between fifth and sixth ribs was made with scissors by cutting intercostal muscles. At the beginning, a small incision was made to control the change of intrathoracic pressure. Later, an incision was extended avoiding pericardio-phrenic a. and vein running superior. Additional care was taken to avoid left lung damage. Chest retractor was gently opened to spread the ribs 3-4 cm in width. On the opening, the pericardium was cut along with an attached pericardial fat. The coronary artery was visualized by lightly pressing on the cardiac apex with e.g. sterile cotton tip applicator (Tristate, NY). This maneuver helped to fill the coronary artery with blood for a couple of seconds, showing a visible pulsating bright red structure in the center of the opened field on LV wall. Taper-point, 3/8 circle 11mm needle with 6-0 prolene suture (EPM8776

Prolene, Ethicon) was passed underneath the coronary artery. When placing the ligature under the artery, it was important to use a shallow bite to not to enter deep into the myocardium. At the same time, it was important not to be excessively superficial. Final knot location was based on rat models published by Chen et al.[9] The suture was tied using double throw and locked in position by using the third knot. Occlusion was confirmed by a transiently visible sudden change of anterior wall color to pale. At this stage escaped blood in the area and in the chest cavity was absorbed using disposable surgical spears (Braintree Scientific, MA). The retractor was slowly removed and the ventilator outflow PE tubing was clamped for two cycles ensuring full lung re-inflation. The chest cavity was closed using taper-point cutting 1/2 circle, 17mm needle with 4-0 nylon (N1245 Nurulon, Ethicon) suture. The chest was closed by bringing together the 5th and the 6th ribs (with pressure applied to the chest wall to reduce the volume of free air). The pneumothorax was eliminated by using sterile catheter and syringe by further evacuation of the air through small chest opening, later closed by the monofilament suture. Muscle layer and skin was closed with 6-0 absorbable and nylon sutures, respectively. About 15-20% mortality following this procedure was anticipated. Pre-warmed sterile isotonic fluids were administered intraperitoneally to help recover blood loss and to keep the rat warm. Analgesic (Buprenorphine, 0.05 mg/kg) was administered shortly after by s.c. injection, then every 8 h for the next 48-72 h. The rat was placed in a quiet low-traffic area away from the operation room, warmed up using the infrared heating lamp. Rats were checked every 10-15 minutes and turned from side to side until fully recovered. It has to be noted that after a period of time adhesions of the fibrous pericardium and mediastinal pleura can occur changing the long axis position of the heart. The author observed fewer adhesions and foreign body responses at 28 days post-MI in cases when monofilament sutures were used to provide an ischemic infarct and also on the closing of the chest cavity. If regular silk was used for both, adhesions were superior, mostly due to its early swelling (blood and tissue fluid) likely due to the higher surface area to volume ratio as indicative of induction of a greater inflammatory response on the braided silk reported earlier by Setzen et al.[25] Fibrous encapsulation at the adhesion sites was also noted in cases when braided silk was used.[25]

2.5. Acute LV Hemodynamic Measurement by Invasive Pressure-Volume (PV) Catheter

Two catheterization rodent-specific approaches can be used to interrogate the pressure and volume in the LV. Closed chest approach is mostly performed through cannulation of the right carotid artery (RCA), while the open chest catheterization is done by entering the chest cavity through fully opened diaphragm. To note, in both cases it is advantageous to use the controlled mechanical ventilation to be able to adjust tidal volumes and respiration rate as procedure requires longer time and precise blood gases and anesthesia control in cases of an unexpected hemodynamic crisis. This article characterizes an open chest catheterization approach while advantages and disadvantages of both catheterizations are later provided in discussion. To note as during closed chest catheterization, use of the echocardiography to guide PV catheter to its final destination is advisable, particularly in cases of remodeled LV apex by thinner scar.

Rats were pre-anaesthetized in the induction chamber and kept on 2% of Isoflurane anesthesia. At this time tetrapolar PV micro-manometer catheter (1.9 F; Transonic Scisense Inc., London, ON) was inserted into a syringe with warm 35-37 ˚C isotonic saline to allow pressure sensor to pre-soak for ~20 min before its use and calibrated. At this time 2 point electronic calibration of volume, phase and magnitude channels took place. Basic four channel IX-404 (Iworx, Dower, NH) A/D recording hardware using compatible PV module software was used to capture, store and later analyze PV recordings. Open chest surgery was performed while animals were secured in dorsal recumbence on the heating pad. The wide V-shape skin incision was made towards the xiphoidal process starting from the right lower thorax quadrant/upper abdomen area. Abdominal wall, skin, and abdominal muscles were carefully retracted and dissected not to injure other organs in the area. The diaphragm was cut through to expose the heart apex, avoiding incisions around sternum to limit bleeding. Cardiac apex was positioned into the diaphragm opening while gently maneuvered using Q-tips. The LV cavity was accessed by means of an apical stab using the 24G needle with outer diameter OD=(0.57mm). The 23G needle OD is (0.64mm) and based on author's experience creates larger than the necessary opening to successfully pass the 1.9F PV catheter that has OD of 0.63mm. As the LV stab is performed on moving the heart, apex needs to be temporary controlled using the Q-tip. The stab was under direct visual control directed along LV long axis by inserting the needle into the cavity with blood found in the needle conus, a sign of successful stab. The surgical microscope can be handy at this time to locate the stab wound. As the needle is withdrawn from the LV cavity by the non-dominant hand, at the same time the insertion of PV catheter can be accomplished by using surgeon's dominant hand to limit the bleeding. The catheter was inserted using its tip to locate the apex stab, while the non-dominant hand was still holding the apex using the needle to partially slow down the contractile movement of the apex and straightening the insertion point.

Standard segment length of PV catheter 8mm for the baseline studies was selected based on measurements of the LV long axis of SD rat. In this study, the LV measured ~10mm. As LV chamber remodeled post-MI and also based on the assessment of long axis using echocardiography at day 28, a catheter with longer segment was selected to accommodate the remodeled chamber. Please see (Table 2) for rat PV catheter segment selection. As PV catheter was fully inserted into the LV it required minor positioning along the long axis of the LV with its later stabilization in place to acquire the best signal. PV catheter position in the LV was constantly observed and adjusted using software-displayed sinusoidal traces of phase angle (ɵ) and admittance magnitude (ϒ). The ranges for a rat were used based on (Table 3), before performing the baseline scan. Additionally, plotting LV pressure vs. LV magnitude, PV loops had the visual characteristic of "toast-like" shape. Baseline scan was performed to obtain live-volume recording by turning the ventilator off for 15-20sec, to obtain HR, end-systolic and end-diastolic blood raw

magnitude values that were displayed using ADV500 control unit (Transonic Scisense Inc., London, ON). After baseline scan, confirming displayed ES, ED and HR values, the LV volume was displayed live on the computer screen. The ventilator was turned off in the inspiration phase, and LV pressure signal stabilized, limiting noise signal coming from the rhythmic movement of the chest cavity resulting in breathing artifact. Temporary turning off the ventilator also allowed PV catheter to get more stabilized along the long axis of the LV. At this point, load dependent "steady state" pressure volume values were recorded. Steady state data were constantly recorded while 30 PV loops samples were offline monitored to ensure overall data consistency. After a period of about 20 min of stable collection of open chest PV load-dependent data, the surgical procedure was commenced to isolate inferior vena cava (IVC) to perform temporary preload reduction maneuvers to obtain load-independent values of the cardiac function. Figure 4 and 5 describes options where to position the occluding suture. As thoracotomy was performed, and the IVC is localized directly below heart in the chest, 6-0 prolene suture was placed under the IVC as it was carefully separated from its adventitia. It is recommended to carefully separate the adventitia as the suture should be placed directly on the vein, without or with very low amount of adventitia. Please note, braided silk is not a perfect material to perform this task, mostly due to its "memory" as it usually swells and then it tends to be more intimately wrapped around the vein after occlusion(s) limiting the preload post-suture release. For this reason, monofilament material might be a better option. Good preload reductions were achieved using occlusion of inferior vena cava (IVC) as proximal possible, away from the heart by slowly lifting the suture upward and cranially, further details are described in the discussion section. The small animal ventilator was shut down for a few seconds before and throughout the whole occlusion to acquire data without lung motion artifacts. This procedure was repeated at least 3 times with pauses, permitting Left ventricle pressure (LVP) and HR to recover to the pre-occlusion values. All traces i.e. Left ventricle pressure, volume, phase, and magnitude signals were observed on the computer screen. In the case of LVP and LVV, both correspondingly declined downwards, while phase tracings followed the opposite direction as it was registering increased proximity of the endocardium as blood was leaving the LV and the chamber was steadily emptying. Attributes of good IVC occlusion is detailed in the discussion. Later, the experiment was terminated by euthanizing the animal using anesthetic drug overdose. PV catheter was carefully removed from the chamber through the stab wound and inserted into 5ml pre-filled syringe with a 0.5% solution of enzymatic non-detergent cleaning solution (Terg-a-zyme, Alconox, White Plains, NY) for at least 30 min. In the case of presence of a visible clot on the catheter, a 2% solution was made up and the catheter was left soaking overnight.

Statistics: All statistics was performed using GrapPad Prism (La Jolla, CA) and its upgraded versions using two-way ANOVA for repeated measures. When a significant effect was observed, post hoc testing was done using e.g. Dunnett's test. All tested parameters were tested for difference between means using paired t-test (95% confidence interval). $P < 0.05$ was considered statistically significant (2-tailed). Values for echocardiography and hemodynamics using PV catheter were expressed as Mean±SEM and Mean±SD, respectively. All P values represent summary of (n=10) for echocardiography (n=17 and 12 resp.), for PV hemodynamics and for HW/BW (n=8 and 10 resp.).

Table 2. *Recommended electrode segment spacing on PV catheter based on rat cardiac long axis.*

Recording electrode segment spacing	Shaft outer diameter (OD) in (F)	Recommended cardiac long axis in (mm)	Maximum Volume measured (µl)
6.0 mm	1.9	7.8-9.8	1000
8.0 mm	1.9	9.8-11.8	1000
10.0 mm	1.9	11.8-13.8	1000
VSL (6,8,10,12 mm)*	1.9	8.3-15.0	1000
VSL (8,10,12,14 mm)	1.9	10.3-17.0	1500
VSL (8,11,14,17 mm)	1.9	10.3-20.0	2000

* VSL: Variable segment length. PV catheters, total shaft length 45.7 (cm), have 4 selectable electrode recording distances to choose from to examine cardiac volumes, advantageous e.g. when examining post-cardiac chamber remodeling.

Table 3. *Ranges of rat baseline LV pressure-volume parameters.*

Heart rate (beats per min)	Systolic Pressure (mmHg)	Diastolic Pressure (mmHg)	Phase range angular frequency (degree)	Phase wave amplitude (degree)	Magnitude variation (µS)	Magnitude wave amplitude (µS)
350-450	100-130	1-6	2-6	2	1400-2600	600-1000

3. Results

Parasternal 2D Echocardiography and baseline PW Doppler measurements

Measurements were collected by linear 10 MHz probe at baseline and at 28 days post-MI in 10 baselines and 9 post-MI Fisher F344 inbred rats. M-mode images were taken at mean HR; 428±11 beats per minute (bpm) at baseline as compared to 371±9 bpm at 28 days post-MI. FS percentages ±SEM as further detailed in (Figure 1C and D). Representative images of short axis view at a mid-papillary level as shown for control (1A) with a comparison of myocardial infarction at 28 days (1B). Quantification of post-MI using 2D guidance for M-mode interrogations showed a significant increase in end-systolic and end-diastolic dimensions in case of post-MI as compared to baseline (EDV; 519µl±34 vs. 282µl±13 n=10 and 15 corresp; $P<0.001$) (1E). Rats with an extensive infarct

presented echo-dense areas in the LV myocardium suggesting the occurrence of extensive fibrosis in the anterolateral apical walls. On occasion, these areas extended into the inferior wall while preserving the interventricular septum. These findings were later confirmed by using histopathological sections in the midpapillary region (Figure 1F); black bar (1cm) with quantification of the ratio of HW/BW in (g/mg) (Figure 1G); (3.1±0.22 vs. 3.82±0.39; P<0.001), reflecting hypertrophy of remaining myocardium.

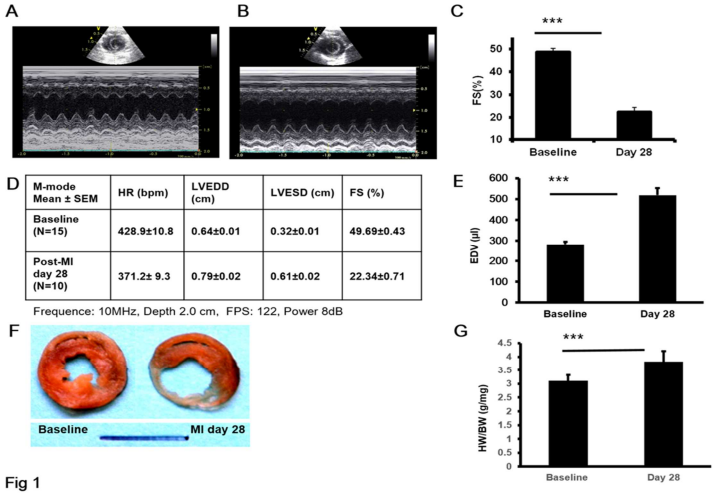

Fig 1

Figure 1. *(A) Image of parasternal M-mode short axis view at the mid-papillary level at baseline and (B) at 28 days post-myocardial infarct. (C) Fractional Shortening (FS) in (%) shows the difference between baseline and 28 days post-MI (***P<0.001). (D) Tabulated M-mode results for LVEDD (cm), LVESD (cm) and FS (%); (E) EDV using calculation out of short axis view baseline and 28-day post-MI (***P<0.001). (F) Representative rat coronal heart section from mid-papillary level; black bar 1cm. (G) HW/BW (***P<0.001).*

Measurement of aortic outflow was done at the longitudinal parasternal long-axis view as per drawing at (Figure 2A), ensuring that aortic cross section area does not change significantly during the flow period to be accurately captured using a 2D image, where the flow profile is likely to be flat[24]. Baselines, obtained from 7 rats, of left ventricle outflow (LVOT) in the area of the aortic annulus, was measured during systole from the two-dimensional images (Figure 2B) and tabled (Figure 2C). Velocity time integrals (VTI) were recorded using pulse wave (PW) Doppler recording through the aortic valve (Figure 2C). All measurements were done in triplicates using manufacturer software for later calculation of stroke volume (SV) using formula (Figure 2E; eq.3) based on publication[23,24]. Baseline SV value from the table 2D was later added into ADV500 control unit as one of the calibration parameters for baseline PV recording. Similarly, at day 28 post-MI, SV can be calculated and added (not shown).

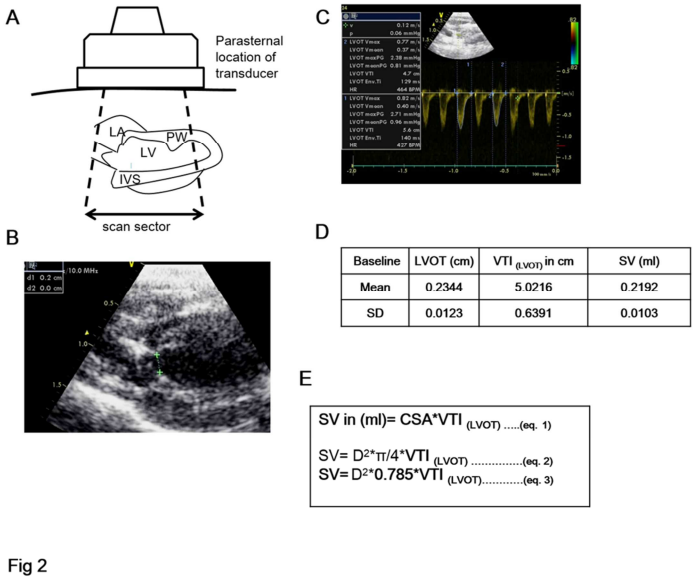

Fig 2

Figure 2. *(A) Sketch of the parasternal location of the transducer when measuring the long axis aortic outflow in a rat model. (B) Representative image of the long axis outflow while measuring the aortic outflow in the area of the aortic root. (C) Representative image of LVOT velocity time integral (VTI) calculation using analysis software provided by Vivid 7 GE echo package. (D) Tabulated baseline values of LVOT and LVOT (VTI) and SV in (ml) by using the SV formula (E).*

Pressure-Volume (PV) hemodynamics Assessment of post-infarction hemodynamics was performed at baseline (n=17) and at 28 days post-MI (n=12) recorded by the open chest technique at 20 min post-stabilization. Analysis of the load dependent hemodynamics at 28 days post permanent suture ligation showed a continuous rightward shift of PV loop on the volume axis, characterized by an increase of LVEDV (319±73 vs. 215±79 µl; P<0.001) and the LVESV (157±39 vs. 57±28 µl; P<0.001) (Fig 3A and D). LV pressure possesses an ultimate effect on the blood propulsion through the LV cavity and into the major artery (ies), and in the case of remodeled LV, it was influenced by the loss of contractile myocytes. As the LV chamber underwent remodeling, both dpdtmax and ESP significantly dropped; dpdtmax (5786±1443 vs. 9609±4126 mmHg; P<0.01) and ESP (91.5±12 vs. 108.2±13 mmHg; P<0.001) at (Fig 3A and B). Both had an effect on the cardiac output and ejection fraction observed at 28 days as compared to controls (Fig 3C and E) (49±12 vs. 68±3.5 ml/min; P<0.05) and (50±8.5 vs. 76±4.9 % P<0.001). Developing diastolic dysfunction had major influence on LV lusitropy at day 28 post MI characterized by prolonged LV filling at higher LV EDP (9.1±2.9 vs. 5.18±2.5 % P<0.01), higher Tau values, time to peak filling (both not shown) and dpdt min (-4850±1062 vs. 5876±1443 mmHg; P<0.001).

A

	Baseline	Day 28
Body weight (g)	275 ± 20	249 ± 44
Heart rate (beats/min)	383 ± 67	360 ± 34
EF (%)	76 ± 4.9	50 ± 8.5 ***
CO (ml/min)	68 ±3.5	49 ± 3.0 *
LV EDV (µl)	215 ±79	319 ± 73 ***
LV ESV (µl)	57±28	157 ± 39 ***
SV (µl)	168 ±51	139 ± 19 *
LV EDP (mmHg)	5.18 ±2.5	9.1 ± 2.9 **
LV ESP (mmHg)	108.2 ±13	91.5 ± 12 ***
dp/dtmax mmHg/s)	9609 ±4126	5876 ± 1443 **
dP/dtmin (mmHg/s)	-7103 ± 2125	-4850 ± 1062 ***

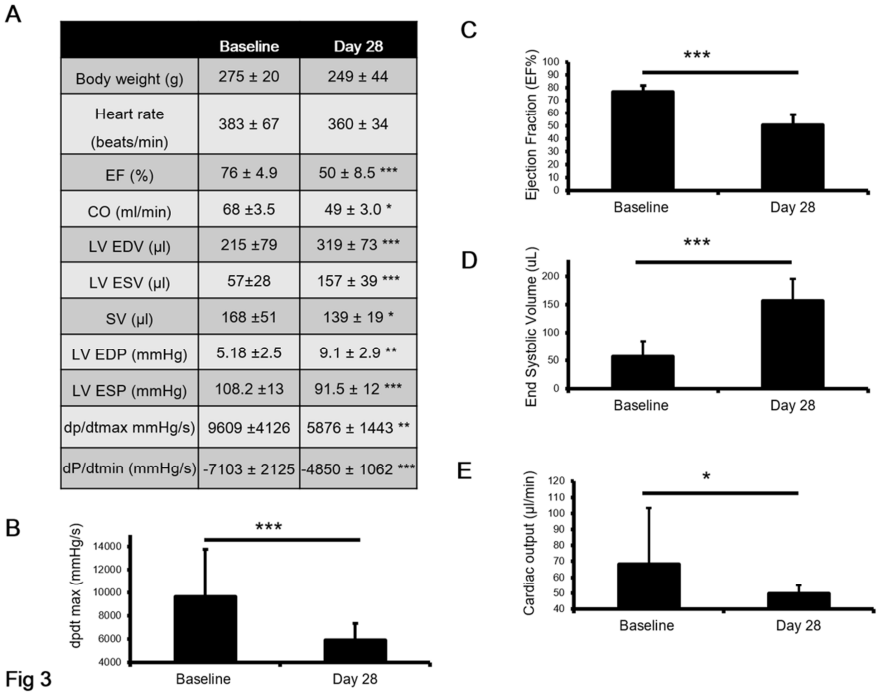

Fig 3

Figure 3. *(A) Table of steady state hemodynamic values collected using pressure-volume (PV) catheter at baseline and post-MI at day 28 from (n=17 and 12 resp.) using two-tailed t-test (***P<0.001; **P<0.01, *P<0.05). Bar graphs of comparison of PV data collected at baselines and at 28 days post-MI (B) dpdt max (mmHg/sec); (C) EF in (%); (D) ESV in (µl) and CO in (µl/min). Statistical significance (***P<0.001) and (**P<0.01) resp.*

3. Discussion

Experimentally induced myocardial ischemia recapitulates symptoms observed in humans as e.g. decrease of exercise tolerance.[26] Modeled infarct size and LV chamber dilation are more pronounced in this model system, whereas other symptoms of heart failure (e.g. pulmonary congestion, dyspnea, and cachexia) are not always fully emergent in a rat. Some authors observe pathophysiological signs such as tachypnea, dyspnea, liver congestion, ascites, pleural-pericardial effusion and ventricular hypertrophy after permanent coronary artery ischemia in a rat.[27] Rat infarcts are usually transmural and are located antero-apically, whereas the inter-ventricular septum and the RV remain unaffected as paralleled to humans. In surviving areas, cardiac myocytes undergo hypertrophy and dilatation, as could be detected by the increase of the ratio of heart weight to total body weight at 28 days, while extracellular matrix supports newly re-modeled chamber's architecture. Larger surviving cardiomyocytes would now have to deliver similar contractile response during the cardiac cycle. Continuous apoptosis further increases the loss of force-generating (contractile) cardiomyocytes leading to uninterrupted dysfunction of systolic load-dependent indices.

Opitz et al[16] reported that larger infarcts sizes are associated with debilitating ventricular arrhythmias in rats. Ventricular fibrillation and tachycardia are occurring mostly at 0-0.5 and 1.5-9 hours post-MI. Their occurrence is deadly in 65% during these two time periods.[16] Others report 6.7% as an early mortality during surgery and at first week post-MI[15] with the infarct size of 33% with death mostly occurring because of respiratory depression, pulmonary edema, and post-infarct arrhythmias.[16,28] Use of e.g. Amiodarone to prevent

arrhythmias in rats induced by halothane-epinephrine during Isoflurane anesthesia was described by Takada et al.[30] Amiodarone is very effective blocking agents to potassium, sodium and calcium channels and have some beta-blocker-like action on the SA and AV nodes. For doses in SD rat post-MI please refer to Morvay et al.[31] Additionally, selection of anesthesia type and the dose is very important when hemodynamics in rodents is interrogated. If there is a choice to plan hemodynamic study in advance avoidance of cardio-depressive anesthetics such as e.g. Pentobarbital, Thiamylal, Thiopental, or a combination of e.g. fentanyl/medetomidine or ketamine/xylazine improves chances to observe closer to physiological ionotropy, lusitropy, and dromotropy. In case injectables cannot be avoided its proper titration needs to be piloted to obtain maintainable levels of HR and blood pressure while performing experimental hemodynamics.

Hemodynamically, at early stages of the myocardial ischemia, peak LV pressures, and dpdtmax are slowly declining as injured LV musculature tries to compensate by temporary decreasing the amount of volume at each stroke at what time ESV is increasing while CO is decreasing, despite all that the heart rate is initially protected. At this time SW is decreasing while EDV is partially protected but soon as myocardial reserves are depleted and LV needs to supply blood to systemic vasculature, diastolic filling-time shortens and EDP starts to rise while dysfunction of LV lusitropy is instigated forcing ventricle to temporary work on low preload reserve and e.g. an intolerance to exercise. As compensatory hemodynamic responses are being exhausted as days on MI are progressing, advancement of systolic dysfunction occurs. Captured by the echocardiography, changes of the LV dilation and chamber's remodeling usually occur at 3-6 weeks post-MI. At that period, already dilated LV cavity is detected using short-axis images at the papillary muscle level, while during post-mortem the hypertrophy of viable cardiomyocytes is confirmed. Literature describes that between 21-28 days post-MI, the degree of LV eccentric hypertrophy increases between 30% and 60%[27] supporting the increase of EDD, ESD and decrease of FS. By frequently used an approximation of volumes using formula (EDV) = $1.047 \times (\text{LVEDD})^3$, a decrease of EF is captured. As short axis volume calculation relies on assumptions of fixed geometric LV shape formula approximation used.[22] Novel recommendations described by Lang et al in 2015 calls for 4 chamber or 2 chamber apical views using biplane method of disks summation correcting for LV shape distortion.[21]

EF in clinical practice is one of the most commonly sought out measurements of systolic-load dependent contractility (ionotropy). By using e.g. echocardiography, EF accounts for cardiac preload by expressing LV SV that is ejected as a fraction of the LV EDV (preload). The EF formula itself does not take into account the afterload (impedance of blood flow) against which the LV has to deliver each LV stroke. This leads to *load-limitation* of myocardial contractility assessment in its entirety as e.g. higher afterloads create adjustments of myocyte ionotropy on the beat by beat basis. In the experimental cardiology, however, the surgeon can temporarily occlude venous inflow e.g. the inferior vena cava (IVC) to assess muscular contractility, closer to the state of the art. The preload reduction has to have certain characteristics (Figure 6). The pre-load maneuver has to be performed at the similar location, using the same vascular occlusion site to compare animal groups (Figure 4 and 5). Moreover, HR at the beginning of IVC occlusion to the end of the occlusion should not be significantly different, the SSE (sum of squares due to error) values that are generated at each beat (here the Max PV ratio) in Figure 6, should possess overall low variability from one beat to the other (in PV dataset created from one IVC occlusion). It is advisable to perform at least 3 IVC occlusions after the HR and LVP stabilize to the levels before each occlusion to allow for multiple ESPVR (end-systolic-pressure-volume) relationship comparisons. When done carefully, results represents one of the gold standards of LV contractility assessment, as other means of contractility measurements, including echocardiography, does not evaluate pressure(s) or provides its beat to beat correlation with LV volume. Similarly, immediately post-occlusion using software functions, the researcher should be able to assess the quality of pre-load reduction as e.g. the end diastolic pressure volume relationship (EDPVR) and others e.g. dpmax vs. EDV that should possess low internal sample variability with high linear regression correlation coefficient (0.7 and higher). Occlusion(s) should be repeated when the internal sample variability is high while the animal is recovering (HR and LVP) to pre-occlusion state. Careful attention has to be paid to HR, LVP values, SSE and R coefficients when analyzing each IVC occlusion. Continuous attention to an animal under anesthesia, reassures well-being of rats and at the same time data reliability, while significantly lowering amount of animals needed in each study arm.

Attributes of repeatable preload reduction by using IVC occlusions during baseline recordings are shown and discussed in Figure 6, additionally: limiting HR variability (if possible i.e. in genetically manipulated) during occlusion to limit activation of e.g. sympathetic nervous system (sinoatrial node augments AV nodal conduction that increases HR). Performed occlusion should be done under close HR monitoring as increasing sympathetic stimulation augments discharge of neurotransmitter norepinephrine (NE) mediating sympathetic response. This neurotransmitter activity sets in motion activation of L-type calcium channels, leading to an influx of calcium into cardiomyocytes, releasing intracellular stores of calcium from the sarcoplasmic reticulum, increasing the amount of calcium available for activation of overall ionotropy. Additionally, premature ventricular contractions (PVCs), at the beginning or during IVC, indicating the necessity to repeat the occlusion. PVCs are relatively common events where the heartbeat is initiated by Purkinje fibers in the ventricles rather than by the pacemaker (the sinoatrial node). During the preload reduction, it is recommended to let heart to recover for longer period in-between occlusions to limit the occurrence of PVCs. Other attributes of good preload reduction have to be summarized in future into standard

procedures, similar to these currently existing in echocardiography, to address load-independent maneuver for each animal species accompanied by basic data analysis guidelines.

After ~ 4 to 6 weeks, based on the severity of the initial coronary artery occlusion, progressive loss of LV ionotropy is observed using PV catheter. As remaining myocardium becomes compensating for constant post-infarction remodeling drop of both, LV systolic and diastolic parameters occur, setting stage for the heart failure (HF) development. Modern collected works of HF introducing remodeling as replacement of necrotic or apoptotic myocardial tissue with fibrotic tissue that is less ionotropic, dromotropic while lacking lusitropy. As the breakdown of nascent cardiac architectural skeleton occurs, individual cardiomyocyte syntitia collapse, leading to a decrease of LV extensibility, resilience, and elasticity. This unique and fast paced hemodynamic adjustment leads to frequent phenotypic signs and symptoms detectable by PV hemodynamics. Data collected at 4 weeks from SD rat during HF helps to identify some of these hemodynamic phenotypic indicators, both load dependent and independent. As e.g. during diastolic dysfunction, alterations of both, relaxation and compliance occur. Relaxation of the LV under myocardial ischemia is impaired in energy-deficient states, notably during early diastole. After the ejection, most LV inflow occurs at this time, and if inadequate observed shortened phase of isovolumic relaxation with rapid LVP descent (using PV) that can be correlated with E wave, deceleration time (DT) and E/A changes, observed (using mitral inflow PW Doppler echocardiography). LV compliance is also affected as LV is not able to expand with rising pressure in late diastole as its passive distensibility is influenced by fibrotic scar tissue with a variety of rhythm disturbances and remodeled LV inflow and its overall chamber's shape. As on the PV plane diagram (P vs. V) the late diastolic filling is characterized well characterized convex-exponential curve fit function (EDPVR), the early diastole, however, should be characterized by concave exponential curve fit.[32] This final sigmoidal diastolic curve fit would encompass the active early inflow i.e. post-mitral closing (untwist and rebound phase) along with the late passive compliance period (pericardial constraint).[32] In rodents using PV diagrams this phenomenon might not be easily observed as for the very little amount of pressure drop (below zero) as this event of sudden suction is observable in large animal (Figure 6C), being registered in early diastolic filling corresponding to motion of the mitral annulus and incoming left atrial blood through the annulus. More research needs to be done to understand this phenomenon in post-MI remodeled LV chamber to better characterize (twist and rebound), during active relaxation at cases of diastolic dysfunction leading to failure.

Figure 6 characterize this relationship throughout whole IVC occlusion, the use the curve-linear fit was preferred to better characterize whole end systolic pressure-volume relationship (ESPRV). The PV software selects point in the PV loop where the Maximal PV ratio occurs (during each cardiac cycle). Each PV loop represents one cardiac cycle in the LV. The group of points represents the relationship of P vs. V and is expressed as slope, also called the end-systolic elastance (Ees), in this case of the LV chamber. The sum of squares due to error (SSE) helps to further characterize the curve-linear fit of Ees (Figure 6B). To portrait author's procedure standardization of IVC occlusion, it was important to use each set of data from preload reduction to pay attention to: mean occlusion beat sampled, and HR at the beginning and at the end of IVC, the SSE values and the R values for each calculated data point e.g. PRSW etc. The lower the SSE value higher goodness of fit of the Ees slope relationship during each preload reduction. The Intercept (V_0) plays a role in the localization of the minimum chamber's volume. The situation when V=0 can hypothetically occur when the LV pressure in the chamber drops to P_0. Again hypothetically, at that time majority of blood is ejected, while there is the persistent amount of blood that can be referred to as "the post-ejection or residual volume" in the chamber that stays is in chamber post one ejection. This post-ejection amount can be further decreased during e.g. increased ionotropy using e.g. dobutamine challenge. During calculation of the LV elastance, this can also mean that V_0 value (the minimal chamber volume point) cannot surpass into negative numbers when the intercept of LVP is at zero mmHg. Theoretically, during certain preload reduction e.g. when using artificial hemodynamic support devices, when LVP becomes negative (that is $P_0<0$) the suction pressure in the LV might enable V_0 to become negative. Please note, the V_0 (IC) is obtained after preload reduction only, therefore it is different as compared to ESV or minimal LV volume (V_{min}).

Described by Fig 6C as preload into LV is decreased, during cardiac cycles at preload end, negative LV pressures in the LV are associated with LA suction through mitral inflow tract. The red sigmoidal curve below encompasses whole preload maneuver but also all individual loops (small sigmoid below) can be used to show the difference of early phases of diastolic pressure volume relationship (twist and rebound) as compared to the late period of LV compliance limited by pericardial constraint. Red points indicate individual cardiac cycle end diastolic PV relationship EDPVR. Creation of points on the individual loop indicating early diastolic PV relationship is necessary to better characterize diastole during preload.

It is preferable to use the close chest approach in some cases, as e.g. in cases of identifying phenotype (hemodynamics in newly generated genetically modified strains of rodents). While using the close chest technique, one has to pay careful attention to the introduction of the catheter into remodeled LV. On numerous occasions, the author has experienced the catheter tip puncturing through the fibrotic scar tissue during either catheter insertion or during its re-positioning. LVP at this point sharply declines as the first sign of acute hemothorax. Also, the outflow tract is changing position as adhesions of pericardium with thoracic pleura deviates the LV long axis. Catheter's smooth aortic insertion and close-to-axial placement is partially restricted by these

complex chest adhesions. Additionally, while characterizing the phenotype the final IVC occlusion(s) using pre-or post-hepatic IVC occlusion after laparotomy have to be carefully executed and adjudicated. If the hemodynamic phenotype characterization is not the ultimate goal of the study, open chest approach can be in many cases a good strategy as e.g. during severe adhesions seen echocardiographically beforehand. Position and insertion of the catheter might be better controlled as the full access to the LV apex is cleared from complex chest adhesions and the LV axis is straightened. Visualization of the scar and the area of viable myocardial tissue helps with decision making during catheter insertion. It is very important to decide how to best insert the catheter for its later ability to be positioned as close to the LV long axis. As for the scar development based on rat coronary artery anatomy discussed earlier, the final scar usually develops while covering the apex, with paraxial vital borders. Given that in both cases all electrodes on PV catheter have to be fully inserted into the cavity, the surgeon has to decide on a) development of technique to safely insert and position/reposition of the catheter through the vital border and b) site of ligation vs. final scar size. Both could be better controlled if the chest is opened on a small pilot study. Additionally, apical insertion usually avoids catheter being entrapped in chordae tendinae, trabeculae or papillary muscles. Both catheter insertion techniques need to be developed with attention to any, even trivial details, which could influence the final hemodynamic outcome(s) and ought to be properly discussed it in material and method section. Discussion of proper preload reduction procedure using IVC occlusion has to be defined to ensure technique repeatability. Moreover, as more and more articles are being published discussing e.g. the ESPVR that has been observed to exhibit nonlinearity and dependence on afterload,[29] need for IVC method and its proper description is extremely important. It was far from the scope of this article to discuss load-independent results of the experimentation on SD rats, with the hope it can be published on another occasion.

The article's main purpose was to present knowledge and share some tips and tricks how to ensure that data obtained have quality checks along the way to properly inquire about hemodynamic and its pathophysiology using rodent HF model system. Presented was e.g. that performed preload reduction should be done under close HR monitoring as increasing sympathetic stimulation augments discharge of neurotransmitters mediating unwanted sympathetic response during preload maneuvers. Additionally e.g., that turning of off the ventilator allows PV catheter to get more stabilized along the long axis of the LV and that location of the catheter during the preload occlusions has immense importance in overall detection of pure cardiac muscle contractility to be fully repeatable and usable in future research and translations into clinical studies. Also briefly discussed was a capacity of PV loop to discern and compare characteristics of early and late diastolic filling i.e. the untwist and rebound phase along with the late passive compliance period (pericardial constraint) that all finding its way into clinical translations e.g. in heart failure with preserved ejection fraction (HFpEF) studies.[33]

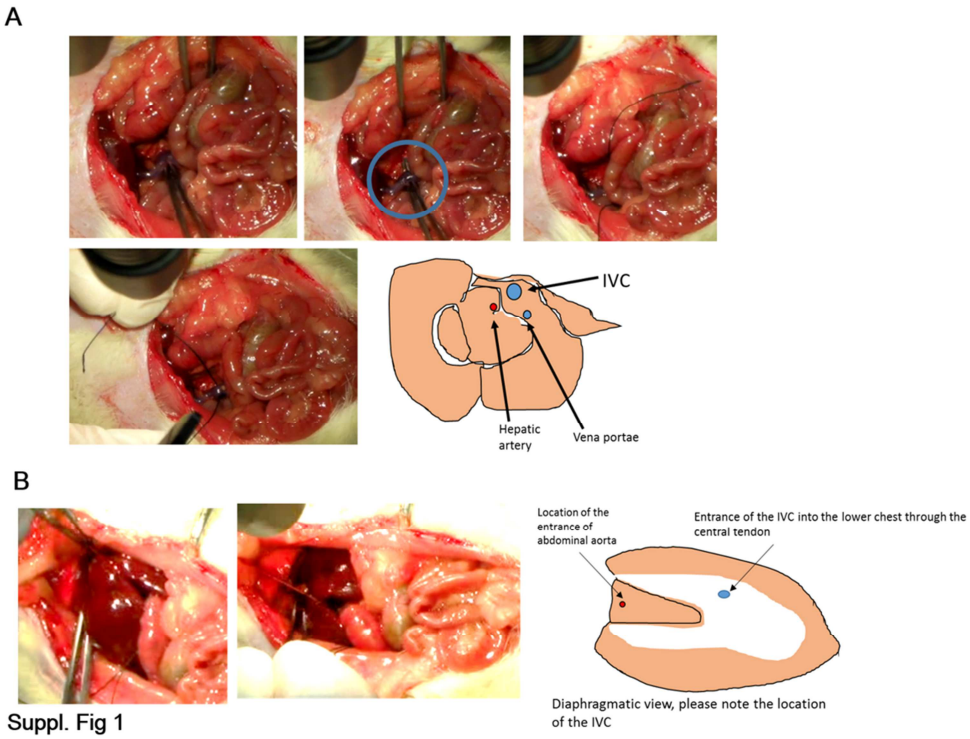

Figure 4. *(A) Post-hepatic location of inferior vena cava (IVC), represents more common location of preload reduction. On the set of pictures from the left, the surgical steps are shown of how to locate the IVC and place occlusion suture around it. To ensure careful suture positioning, please see a drawing of the location of vena portae. (B) Pre-hepatic location of IVC. Rat is positioned in dorsal recumbence while attached drawing shows the location of the IVC as it enters through the central tendon of diaphragm. The liver needs to be carefully separated and pulled away using atraumatic techniques to limit bleeding.*

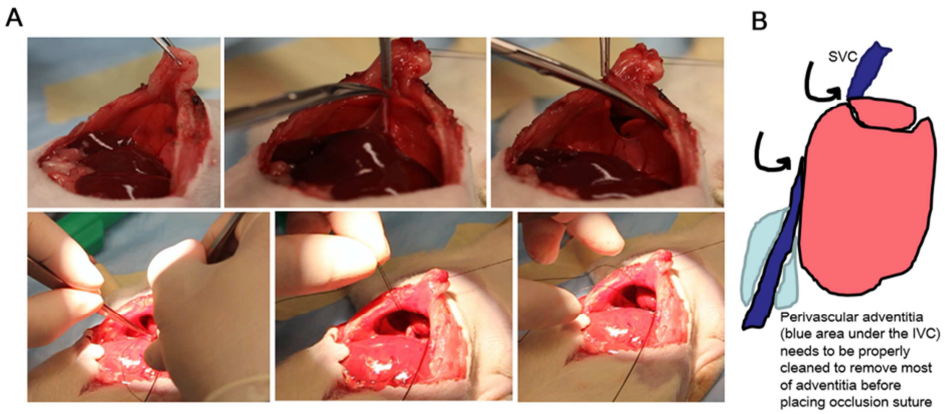

Figure 5. *(A) Set of pictures starting from top left describing thoracotomy. The chest is opened in dorsal recumbence (upper row from the left). Forceps are used to hold the xiphoid while Metzenbaum scissors carefully opening the diaphragm avoiding cutting into the lung parenchyma. Sometimes tension suture positioned through the xiphoid helps with diaphragm dissection. Bottom row from the left: after diaphragm, opening IVC can be located below the RV and it is very easy to be separated from its adventitia. (B) If separated carefully, the final quality of preload reduction is superior to both techniques (pre- or post-hepatic) shown at Fig 4. Moreover, superior vena cava (SVC) can be also occluded, to compare this preload maneuver with IVC only.*

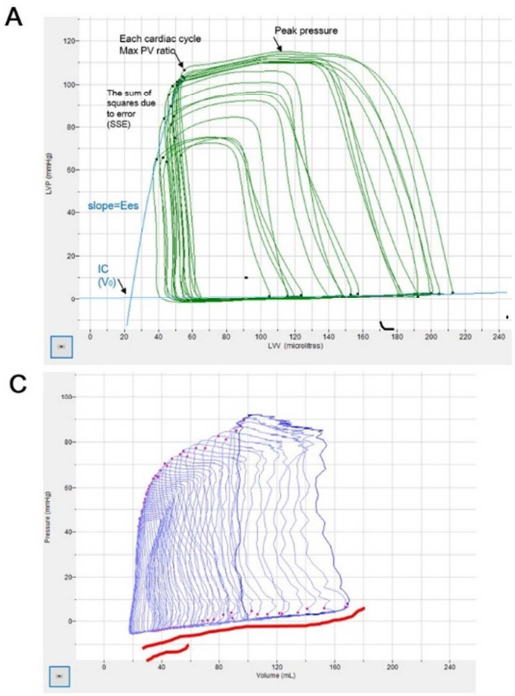

B

	Baseline
ESPVR	EXPONENTIAL
IC (V_0)	25.54
Slope (Ees)	5.67
mean occlusion beats sampled	35.67
IVC Heart Rate start	355.17
IVC Heart Rate end	352.50
SSE	1363
EDPVR	EXPONENTIAL
Stiffness	0.10
Max dpdt vs. EDV	LINEAR
R	0.960
Slope (Ees)	29.011
sampled delta Pmax-end	40.330
P max	122.070
E max	2.620
at mSec post EDV	70.200
PRSW	LINEAR
R	0.990
IC (V_0)	91.870
Slope (Ees)	123.450

Figure 6. *(A) As the LV venous return decreases, in this example into the LV, using temporary occlusion of IVC post-thoracotomy, the maximal PV ratio and thus individual elastances decreases as chamber ejects blood through the aorta at every cardiac beat. Given the stable afterload, amount of blood ejected from the LV at every cardiac beat (during preload reduction) is not leaving the chamber linearly as compared to LVP, but rather leaves faster at the beginning. driven by LVP, LVV is decreasing more rapidly during first milliseconds after the Aortic valve opens. (B)Data table includes representative means of load-independent data from baselines (n=6). C) Characteristics of early and late diastolic phases during multiple cardiac cycles (using large animal example of preload reduction) to better illustrate the phenomenon.*

Conflict of interest

None declared.

References

[1] Arbustini E, Dal Bello B, Morbini P, et al. Plaque erosion is a major substrate for coronary thrombosis in acute myocardial infarction. *Heart.* 1999; 82(3): 269-72.

[2] Heimburger RF. Injection into pericardial sac and ligation of coronary artery of the rat. *Arch Surg.* 1946; 52: 677-89.

[3] Kaufman N, Gavan TL, Hill RW. Experimental myocardial infarction in the rat. *AMA Arch Pathol.* 1959; 67(5): 482-8.

[4] Selye H, Bajusz E, Grasso S, et al. Simple techniques for the surgical occlusion of coronary vessels in the rat. *Angiology.* 1960; 11: 398-407.

[5] Pfeffer MA, Pfeffer JM, Fishbein MC, et al. Myocardial infarct size and ventricular function in rats. *Circ Res.* 1979; 44(4): 503-12.

[6] Ader R, Chatterjee K, Ports T, et al. Immediate and sustained hemodynamic and clinical improvement in chronic heart failure by an oral angiotensin-converting enzyme inhibitor. *Circulation.* 1980; 61(5): 931-7.

[7] Packer M, Medina N, Yushak M. Comparative immediate hemodynamic and hormonal effects of amrinone and captopril in patients with severe chronic heart failure. *Am J Med Sci.* 1986; 291(1): 8-15.

[8] LeJemtel TH, Keung E, Frishman WH, et al. Hemodynamic effects of captopril in patients with severe chronic heart failure. *Am J Cardiol.* 1982; 49(6): 1484-8.

[9] Chen J, Petrov A, Yaniz-Galende E, et al. The impact of pressure overload on coronary vascular changes following myocardial infarction in rats. *Am J Physiol Heart Circ Physiol.* 2013; 304(5): 719-28.

[10] Liu YH, Yang XP, Nass O, et al. Chronic heart failure induced by coronary artery ligation in Lewis inbred rats. *Am J Physiol.* 1997; 272: 722-7.

[11] Pfeffer MA, Pfeffer JM, Steinberg C, et al. Survival after an experimental myocardial infarction: beneficial effects of long-term therapy with captopril. *Circulation.* 1985; 72(2): 406-12.

[12] Huwer H, Winning J, Vollmar B, et al. Model of chronic systolic and diastolic dysfunction after cryothermia-induced myocardial necrosis in rats. *Comp Med.* 2000; 50(4): 385-90.

[13] Li RK, Mickle DA, Weisel RD, et al. Optimal time for cardiomyocyte transplantation to maximize myocardial function after left ventricular injury. *Ann Thorac Surg.* 2001; 72(6): 1957-63.

[14] Costa AR, Panda NC, Yong S, et al. Optical mapping of cryoinjured rat myocardium grafted with mesenchymal stem cells. *Am J Physiol Heart Circ Physiol.* 2012; 302(1): 270-7.

[15] Jin J, Jeong SI, Shin YM, et al. Transplantation of mesenchymal stem cells within a poly(lactide-co-epsilon-caprolactone) scaffold improves cardiac function in a rat myocardial infarction model. *Eur J Heart Fail.* 2009; 11(2): 147-53.

[16] Opitz CF, Mitchell GF, Pfeffer MA, et al. Arrhythmias and death after coronary artery occlusion in the rat. Continuous telemetric ECG monitoring in conscious, untethered rats. *Circulation.* 1995; 92(2): 253-61.

[17] Konecny F, Zou J, Husain M, et al. Post-myocardial infarct p27 fusion protein intravenous delivery averts adverse remodelling and improves heart function and survival in rodents. *Cardiovasc Res*. 2012; 94(3): 492-500.

[18] McPherson R, Pertsemlidis A, Kavaslar N, et al. A common allele on chromosome 9 associated with coronary heart disease. *Science.* 2007; 316: 1488-91.

[19] Helgadottir A, Thorleifsson G, Manolescu A, et al. A common variant on chromosome 9p21 affects the risk of myocardial infarction. *Science.* 2007; 316: 1491-3.

[20] Klocke R, Tian W, Kuhlmann MT, et al. Surgical animal models of heart failure related to coronary heart disease. *Cardiovasc Res.* 2007; 74(1): 29-38.

[21] Lang RM, Badano LP, Mor-Avi V, et al. Recommendations for cardiac chamber quantification by echocardiography in adults: an update from the American Society of Echocardiography and the European Association of Cardiovascular Imaging. *J Am Soc Echocardiogr.* 2015; 28(1): 1-39.e14.

[22] Brown L, Fenning A, Chan V, et al. Echocardiographic assessment of cardiac structure and function in rats. *Heart Lung Circ.* 2002; 11(3): 167-73.

[23] Lewis JF, Kuo LC, Nelson JG, et al. Pulsed Doppler echocardiographic determination of stroke volume and cardiac output: clinical validation of two new methods using the apical window. *Circulation.* 1984; 70(3): 425-31

[24] Quiñones MA, Otto CM, Stoddard M, et al. Doppler Quantification Task Force of the Nomenclature and Standards Committee of the American Society of Echocardiography. Recommendations for quantification of Doppler echocardiography: a report from the Doppler Quantification Task Force of the Nomenclature and Standards Committee of the American Society of Echocardiography. *J Am Soc Echocardiogr.* 2002; 15(2): 167-84.

[25] Setzen G, Williams EF. Tissue response to suture materials implanted subcutaneously in a rabbit model. *Plast Reconstr Surg.* 1997; 100: 1788–95.

[26] Koh SG, Brenner DA, Korzick DH, et al. Exercise intolerance during post-MI heart failure in rats: prevention with supplemental dietary propionyl-L-carnitine. *Cardiovasc Drugs Ther.* 2003; 17(1): 7-14.

[27] Zornoff LA, Paiva SA, Minicucci MF, et al. Experimental myocardium infarction in rats: analysis of the model. *Arq Bras Cardiol.* 2009; 93(4): 434-440.

[28] Fletcher PJ, Pfeffer JM, Pfeffer MA, et al. Left ventricular diastolic pressure-volume relations in rats with healed myocardial infarction. Effects on systolic function. *Circ Res.* 1981; 49(3): 618-26.

[29] Blaudszun G, Morel DR. Relevance of the volume-axis intercept, V0, compared with the slope of end-systolic pressure-volume relationship in response to large variations in inotropy and afterload in rats. *Exp Physiol.* 2011; 96(11): 1179-95.

[30] Takada K, Sumikawa K, Kamibayashi T, et al. Comparative efficacy of antiarrhythmic agents in preventing halothane-epinephrine arrhythmias in rats. Anesthesiology. 1993; 79(3): 563-70.

[31] Morvay N, Baczkó I, Sztojkov-Ivanov A, et al. Long-term pretreatment with desethylamiodarone (DEA) or amiodarone (AMIO) protects against coronary artery occlusion induced ventricular arrhythmias in conscious rats. *Can J Physiol Pharmacol.* 2015; 93(9): 773-7.

[32] Pasipoularides A. Right and left ventricular diastolic flow field: why are measured intraventricular pressure gradients small? *Rev Esp Cardiol (Engl Ed).* 2013; 66(5): 337-41.

[33] Komajda M, Lam CS. Heart failure with preserved ejection fraction: a clinical dilemma. *Eur Heart J.* 2014; 35(16): 1022-32.